Applied Energy Symposium 2021: Low carbon cities and urban energy systems
September 4-8, 2021, Matsue, Japan
Paper ID: 47

Investigation of the novel integration of mashrabiya and heat transfer devices for buildings in hot climates

Abdullah Abdulhameed Bagasi[1,2], John Kaiser Calautit [2]
1 Department of Islamic Architecture, Umm Al-Qura University, Makkah, Saudi Arabia (Corresponding Author)
2 Department of Architecture and Built Environment, University of Nottingham, Nottingham, NG7 2RD, U.K.; aabagasi@uqu.edu.sa (A.B.); John.calautit1@nottingham.ac.uk (J.C.)

ABSTRACT

This paper investigates the novel integration of heat transfer devices into a mashrabiya device to improve indoor thermal comfort conditions in buildings in hot climates. The benchmark case building model was validated using detailed wind tunnel data based on particle image velocimetry (PIV) and Computational Fluid Dynamics (CFD) modelling results. Good agreement was observed between the modelling results and previous works data. Then, three configurations were evaluated: a) base case, b) single row of heat transfer devices, and c) double rows of heat transfer devices combined with the mashrabiya. The results of the building with mashrabiya indicated that the slats' inclination plays a vital role in the airflow distribution in the room, and this was evident with tilting the slats angle to +30° or -30°, as the airflow became more directed and sharper towards the ceiling or the floor. Also, as compared to the benchmark case, the mashrabiya contributed to increasing the airflow rate into the room. Overall, the addition of heat transfer devices decreased the temperature by up to 7.5°C (18.8%).

Keywords: Computational fluid dynamics (CFD), mashrabiya, energy conservation in buildings, natural ventilation, heat transfer, thermal comfort.

1. INTRODUCTION AND LITERATURE REVIEW

With the economic boom in Saudi Arabia, many developments occurred in different sectors, including urban development and construction. However, that caused the emergence of some issues in modern buildings where the buildings became more reliant on active systems, especially ventilation, instead of optimising natural resources, which has led to increased energy consumption. Besides, most of the modern buildings have lost their local and original architectural identity. Combined with the hot climate in Saudi Arabia, these factors have contributed to the increase in energy use in modern residential buildings, consuming about 50% of the generated energy. The Saudi Energy Efficiency Center indicated that in 2020 about 70% of electricity consumption in residential buildings was often attributed to air conditioners.

Traditionally, the local residential buildings in Saudi Arabia were characterised by different architectural solutions and elements such as the mashrabiya, which was closely related to the local environment and responded to many factors, such as climatic conditions and occupants needs. Mashrabiya was described by Bagasi and Calautit [1] as an opening covered with a wooden lattice for ventilation, daylight, privacy, and an aesthetic appeal for houses. Several studies have been conducted to revive the mashrabiya with several solutions and methods in recent years.

Some studies included validation procedures without integrating cooling techniques as [2], [3], [4]. In contrast, [5], [6], [7] studied the effect of mashrabiya integrated cooling techniques without covering the validation procedures. Although Ramponi and Blocken [8] model was designed as an isolated building with two openings without mashrabiya or cooling technique, it presented a simplified and accurate model similar to experimental results through extensive study of many parameters and variables in CFD, which was adapted as a reference case for this study. Moreover, the studies of [2], [3], [4], [5], [9], and [10] were taken advantage of, specifically in identifying some variables or methods of analysis used.

Selection and peer-review under responsibility of the scientific committee of CUE2021

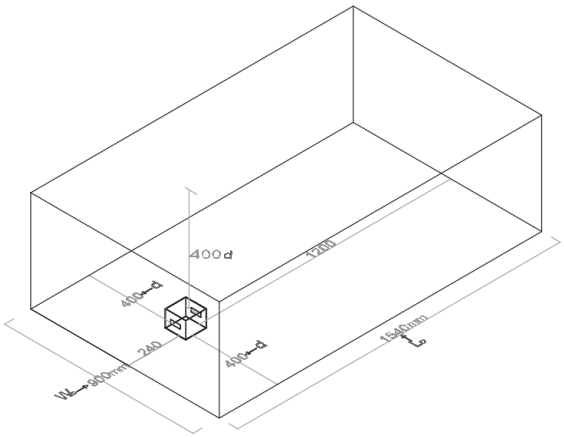

Fig 1 The dimensions of CFD domain and base room model.

2. METHOD

2.1 Model Validation

To the best of our knowledge, simulated a valid cross-ventilation model with cross ventilation has not been studied or investigated. Therefore, this study required firstly a valid model based on an isolated building with two openings without mashrabiya or cooling technique. Based on the selected CFD reference case "RCM" of [8], which relied on the best practice guidelines by Franke, et al. [11] and Tominaga, et al. [12], the computational domain and room position of this work was created as shown in Figure 1.

The domain dimensions in full scale are 180 x 308 x 96 m^3 (W_D x L_D x H_D), and the room is 20 x 20 x 16 m^3 (W_R x L_R x H_R). For simulation purposes, scale 1: 200 was used for this model as recommended in RCM (Figure 1) where the domain became equal to 900 x 1540 x 480 mm^3 and the room 100 x 100 x 80 mm^3.

The tetrahedral mesh has been used to save computing time and preparing for the solver. The volume mesh size was determined at 0.015 m and set the facing size at 0.0007m for the room, defining hard as behavior. Accordingly, the cell elements amounted to 6,836,946 with nodes 1,256,350 with an average skewness and aspect ratio of 0.224 and 1.84, respectively.

The boundary conditions used in the simulations were based on Ramponi and Blocken (2012) data of the vertical profile of mean wind speed, as seen in Figure 2 (A). It was mentioned by Ramponi and Blocken [8] that "A reference mean U_{ref} wind speed of 6.97 m/s and a reference turbulence intensity of 10% was measured at building height", where the dashed line shows the height level of the building or room. Since there were no exact or clear measurement points was found from the [8] for the curve of the reference mean wind speed profile, the curve in Fig 2 (B)has been re-drawn by matching the same curve as closely as possible and reusing it in this work and therefore this may result in some slight differences in the validation results.

Figure 3 illustrates the flow domain of the computational model showing the boundary conditions (inlet, outlet, ground, Symmetry) and their positions

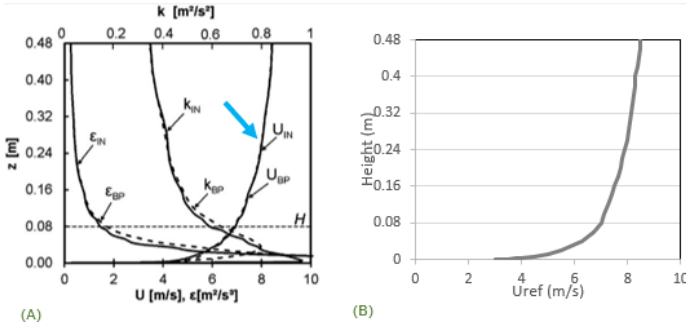

Fig 2 (a) Profiles of the mean wind speed (U) from RCM and the U_{ref} applied in this simulation.

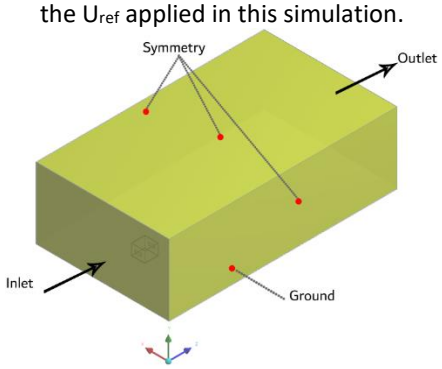

Fig 3 The boundary conditions in the flow domain of the computational model.

concerning the axes. At the outlet plane, the static pressure of the outlet and symmetry conditions was set on zero, and the symmetry conditions domain means that zero normal velocity and zero normal gradients of all variables at symmetry planes [8].

The simulations were conducted with the commercial CFD ANSYS FLUENT 18.1 to simulate the airflow inside the domain and into the room. Different iterations were applied 1000, 2000, and 10000 to obtain the best convergence and lowest residuals. All iterations of each case were run and completed without errors.

In addition, the SIMPLE algorithm was used with the default setups of ANSYS, where the pressure and momentum were specified second-order.

The 3D steady RANS equations are solved in combination with three turbulence models; (1) Shear Stress Transport (SST k- ω) model, standard k-epsilon (k-ε) model, (3) RNG k-epsilon (RNG k-ε)model;(4) K-omega (k- ω) model.

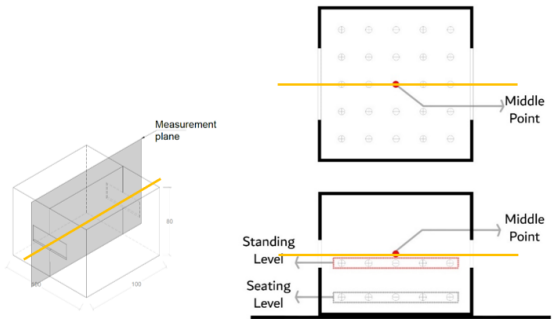

Fig 4 CFD measurements levels and points.

It is worth noting that several points in two different levels have been specified to measure the average of airflow inside the room has been shown in Figure 4. One midpoint and two different levels were taken as the averages of indoor airflow; One is 34mm high, and the other is 12mm off the floor. Each level contains 25 points with an equal distance of 17.5 mm around each point. Besides that, the middle line is the main measurement reference for comparing the results with wind tunnel data of the PIV and CFD reference case "RCM", while the plane was a section measurement for air velocity.

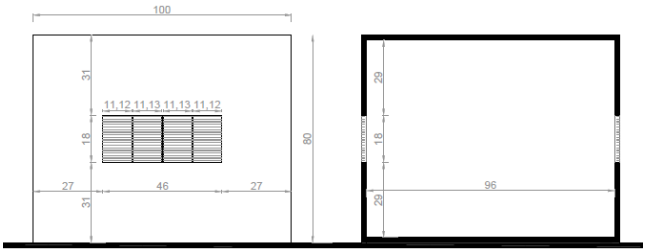

Fig 5 The computational room in the base case.

2.2 *Base Case*

After creating a validation model, the base case was created based on the benchmark case, adding a plain mashrabiya in both openings. This stage aimed to investigate the effect of cross ventilation of the room with two opposite mashrabiyas. Moreover, define the most effective inclination angle in the mashrabiya of airflow into the room. The geometry of this case was created based on the benchmark model and included a plain mashrabiya was added, whose ratios were derived from the sizes of the mashrabiya slats and sashes tested by [1], while benefited from [2] to determine the angles of the slats.

Two plain mashrabiyas were added to the room's openings, one facing the windward and the other the leeward facade, as seen in Figure 5. Each mashrabiya consists of 4 sashes where the mashrabiya dimensions are 46 x 18 mm at the height of 31 mm, corresponding to 9.2 x 3.6m3 in full scale. In addition, five configurations of slats inclination angles were tested; horizontal, +30°, -30°, +20°, -20°.

The base case used tetra mesh, k-ε standard model, and U_{ref}=6.97 m/s as a mean wind speed profile while the same boundary conditions were applied as was applied on the benchmark case. However, due to adding the mashrabiya, the cell elements increased about 7% from the benchmark case, where it became 7,341,339 with 1,370,881 nodes.

It is worth noting that several points represent either level of standing or seated have been specified based on the ASHRAE standards [13]. These points aimed to find the average airflow inside the room; one midpoint and two different levels were taken as the averages of indoor airflow; One is 1.7m high, and the other is 0.6 off the floor. Besides that, the middle line was set to compare the results.

2.3 *Integration of heat transfer devices with mashrabiya*

This phase principally aimed to investigate the effect of integration cooling pipes with mashrabiya to decrease the indoor temperature and improve comfort. The applied method adopted a system that uses heat transfer devices to provide a continuous cooling cycle, which lowers internal temperatures during hot conditions [14]. Two configurations were carried out with this strategy: a) single row pipes and b) double rows of pipes combined with mashrabiya. The pipes were added behind the mashrabiya that facing the wind. The pipe diameter is 7.5mm, and the length is 1.71mm.

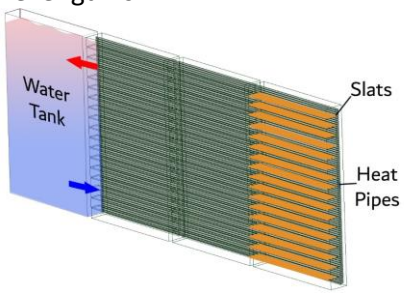

Fig 6 Mashrabiya integrated with pipes and water tank.

In Fluent, the domain a scale of 1:50 to get more appropriate room dimensions and then apply the ASHRAE standard of measurement levels. The slats inclination angles in this phase either were set as horizontal or -20°.

One sash was removed to add a space for the water tank in the windward mashrabiya. Also, one sash was removed in the opposite mashrabiya as well to be of equal sizes. The primary purpose of the water tank was to maintain the set temperature of pipes and not release the generated heat into the room, see Figure 6.

Due to the small size of the pipes, this was required to increase the mesh size and enable the model to run in

the solution, which resulted in cells elements 11,233,810 (single pipes) and 11,809,618 (double pipes). Five different U profiles of the mean wind speed were tested; 5, 4, 2, 1, and 0.5 m/s. In order to study the temperature with airflow, the energy equation in the pipes phases was turned ON with specifying different temperatures. Also, the materials for some parts were defined. Table 1 shows the materials that have been used and their properties. The inlet and outlet temperatures were set at 40 or 30 C°, while the pipes were set at 22 or 17 C°. The same solver settings of the base case were applied in this phase.

Table 1 ain configurations of the geometry of each phase.

Part	**Material**	**Material properties**		
		ρ (Kg/m3)	C*p (j/kg.k)*	**Λ** *(w/m.k)*
Ground	Calcium-carbonate	2800	856	2.25
Room				
Slats	Wood	700	2310	0.173
Pipes	Copper	8978	381	387.6

3. RESULTS AND DISCUSSION

3.1 Model Validation

The result of the benchmark case building was mainly compared with the data of PIV to verify the validity of the model data, while the RCM was considered to confirm the validity of the benchmark case data and its fluctuation within an acceptable range according to those results. Table2 below presents orderly the most compatible cases with PIV to least where the curves represent the measurement line data as displayed in Fig 4. Also, the other criteria used to define the best cases were the error rate and the fulfilment of iterative convergence. The averages airflow results of all cases were on level 0.012m, around 1.39 to 1.8 m/s, and level 0.034m in a range of 1.45 and 2.04m/s.

Case 1-4T was somewhat closer to the PIV based on the grey area in Figure 7; a lack of repeated convergence affected the increase in airflow values in the middle of the room whilst increasing the iterations contributed to more similar results with the PIV. According to the considerations made in the table and charts, 1-6T "K-ε standard model" was the best agreement model to PIV measurements, followed by 1-8T "K-ε RNG". However, it has been proven that the k- ε standard model results with iterations of 2000 (1-5T) gave identical results to 1-6T with an error rate of 1.6% higher, Figure 8. In contrast, 1-5T could save computing time by about 30%. Therefore, the used turbulence model with 2000 iterations was selected as a constant setup for the Fluent in the subsequent phases.

Table 2 The agreement between PIV measurement data and tetra mesh cases.

Case			Iterations	Error (%)	Similarity to PIV chart	Residuals
1	1-6T	K- ε standard	10000	29.3	2	-3
2	1-8T	K- ε RNG	10000	31.4	10	-3
3	1-3T	SST	10000	33.8	8	-3
4	1-10T	K-omega	10000	31.6	5	-2
5	1-5T	K- ε standard	2000	31.9	3	0
6	1-2T	SST	2000	33.2	7	-2
7	1-9T	K-omega	2000	31.6	6	0
8	1-4T	K- ε standard	1000	35.3	1	3
9	1-7T	K- ε RNG	2000	38.3	9	0
10	1-1T	SST	1000	31.2	4	2

Residuals: (3 to -3, where 3 means high residuals and -3 high)

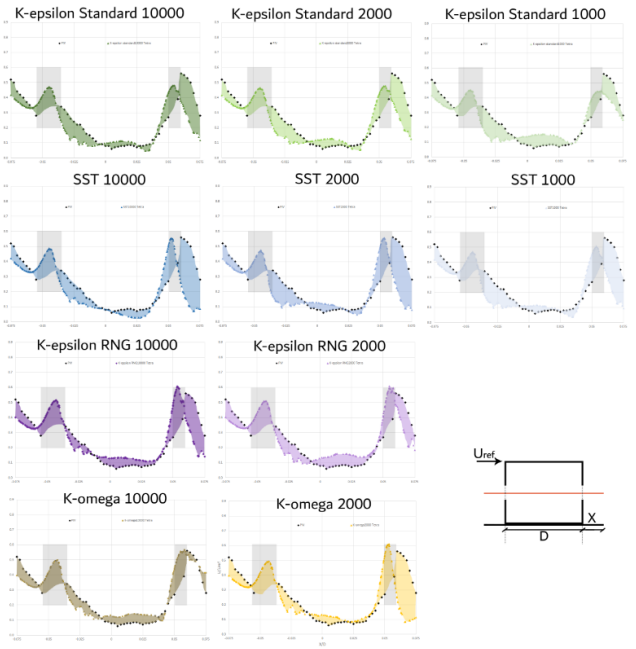

Fig 7 The airflow measurements of Tetra mesh cases comparing to PIV measurement

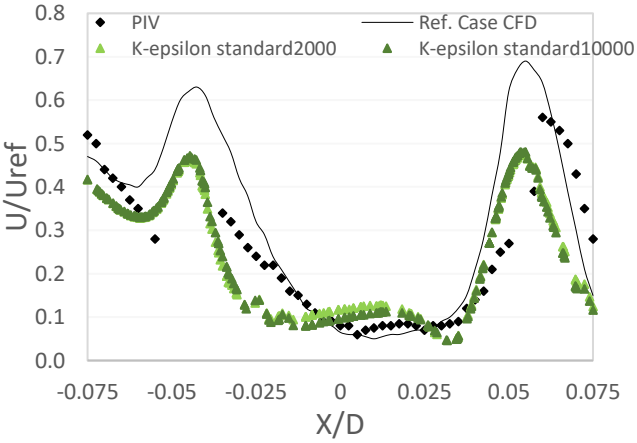

Fig 8 The PIV and RCM curves with comparison the best similar generated cases

3.2 Base Case

Figure 9 presents the cross-sectional plots of the air velocity contours in the room of each model in the base case. It was observed that the greater the inclination of the slats towards the up or down, the lower the airflow rate in the middle of the room and the sharper the angle of the airflow towards the ceiling or floor.

Figure 10 presents the averages of air velocity in the base case for different cases based on the inclination angle of slats mashrabiya. The graph shows the effect of applying five different inclination angles on the averages of air velocity in three different positions. Based on the monitored data in the middle of the room and standing level, the best cases were 2-1 and 2-5 of the velocity distribution efficiency inside the room and were selected for the heat transfer devices stage.

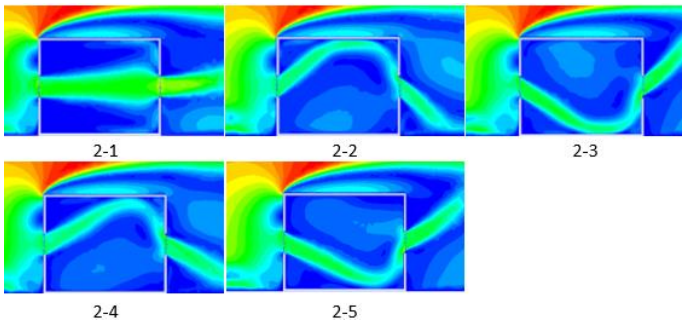

Fig 9 the cross-sectional plot of the air velocity contours in the room for the models in the base case

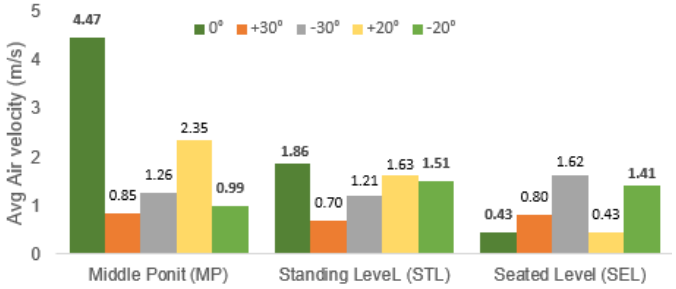

Fig 10 the cross-sectional plot of the air velocity contours in the room for the models in the base case

3.3 Integration of heat transfer devices with mashrabiya

3.3.1 Single row of pipes integrated with mashrabiya

Figure 11 represents the air velocity contours for cases designed with horizontal slats (3-1 to 3-4) and cases with an inclination angle of -20° (3-5 to 3-8). Despite the change in the angle of inclination of the slats in this phase, the similarity of the airflow patterns can be observable due to the adding the pipes.

The result of temperature distribution indicated that the room in this phase was affected by the velocity profile, which allowed high heat transfer, thus limiting the effect of pipes on the room, as the drop did not exceed 1° in the best case when the inlet temperature was set at 40° and pipes on 17°.

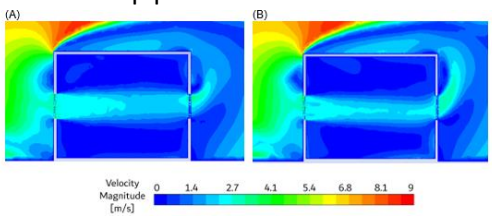

Fig 11 Airflow velocity contours at the measurement plane (A) the model with horizontal slats and (B) inclination angle -20°

3.3.2 Double rows of pipes integrated with mashrabiya

Although tested five wind speed profiles between 0.5 to 5 m/s with two different inclination angles for the slats: horizontal and -20°, the flow patterns were similar in most cases. This is due to the additional row of pipes and thus had a more significant impact on the airflow distribution pattern. Therefore, the angle of inclination of the mashrabiya slats became less effective in forming the air pattern in this phase.

In this phase, the temperature distribution results indicated that with the increase in the inlet airspeed, the effectiveness of the cooling strategy decreases due to the high amount of heat transfer from outside to inside. In contrast, with the decrease in the airspeed profile, the system becomes more efficient.

3.4 Comprehensive comparison of the simulation Phases

3.4.1 The base case vs the benchmark model

Table 3 shows the airflow rates for the standard case compared to the results of adding mashrabiya and its effect on airflow rates when changing the angle of inclination of the slats. It is clear from this that case 2-1 afforded the best airflow at the standing level. In addition, the mashrabiya contributed to the continuity of airflow on the standing level efficiently compared to the benchmark case. Case 2-3 indicates that with the slats inclinations of -30, the mashrabiya provided more flow in the seating area than the benchmark case.

Table 3 the averages of airflow results for the benchmark case and the base case.

Case	Slats angel	(STL)	(SEL)
Benchmark case	NA	1.62	1.44
2-1	0°	1.86	0.43
2-2	+30°	0.70	0.80
2-3	-30°	1.21	1.62
2-4	+20°	1.63	0.43
2-5	-20°	1.51	1.41

3.4.2 Single row of pipes vs Double rows of pipes

By comparing the results of the configurations of the pipes, it was found that the single pipes row had less reduction on the airflow. However, it has been observed that despite the change in the angle of inclination of the slats, the effect of adding pipes, either single row or double, contributed to the similarity of the airflow pattern, as shown in Figure 12. The results of both phases were reflected in the velocity profile used for each case. The cases with the single-pipe row when using the profile of the mean wind speed U_{ref}=6.97 m/s as in the benchmark case indicated a slight temperature drop of less than 1 degree at best case. The mean wind speed profile allowed more heat transfer, thus limiting the impact of the pipes on the room. In the double pipes, the air wind speed profile was tested from 0.5 to 5 m/s, but the flow patterns were similar in most cases due to these additional rows of pipes. Therefore, the angle of inclination of the mashrabiya slats became less effective in forming the air pattern in this phase. Although the addition of another row of pipes reduced the airflow force, this contributed to an increase in the effectiveness of the pipes, which resulted in an apparent reduction in

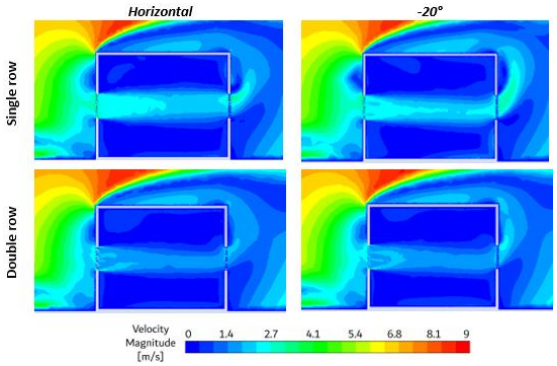

Fig 12 the overall airflow velocity contours at the measurement plane for both pipes phases

room temperatures. Unfortunately, the application of these pipes may cause a lack of daylight and outside visibility.

The air velocity, temperature, and thermal comfort rates for the most effective phase are presented in Table 4. The thermal comfort was specified by using [15] equation as follow;

$$T_c = 0.31\,T_o + 17.8 \qquad (1)$$

From this equation, the calculated comfort temperature was 30.2C°, while the other thermal comfort was set based on the field study [16] that indicated the participants felt comfortable at around 33°C.

This method generally indicated lower temperatures while reducing the reference air velocity profile, reducing heat transfer and increasing system efficiency. When the slats were set horizontally or tilt -20 with a mean wind speed profile U_{ref}=0.5 m/s indicated a temperature decrease of 7.5°C (18.8%), resulting in thermal comfort.

Table 4 the averages of air velocity, temperature, and comfort for the double pipes' cases.

Case	U_{ref}	Velocity	Temperature	Thermal comfort	
		Avg.	Avg.	Ref. *30.2 C°*	Ref. *33 C°*
4-1	5	0.48	38.97	-8.8	-5.97
4-2	4	0.35	38.81	-8.6	-5.81
4-3	2	0.18	38.02	-7.8	-5.02
4-4	1	0.08	36.06	-5.9	-3.06
4-5	0.5	0.04	32.50	-2.3	0.50
4-6	5	0.53	39.00	-8.8	-6.00
4-7	4	0.43	38.86	-8.7	-5.86
4-8	2	0.17	38.06	-7.9	-5.06
4-9	1	0.09	35.90	-5.7	-2.90
4-10	0.5	0.04	32.47	-2.3	0.53

From the results, it can be said that higher air velocities with higher temperatures cause more heat transfer to the room and thus reduce the efficiency of the cooling strategy. Overall, the double pipes with the U_{ref} 0.5 m/s reference velocity profile indicated the highest reduction in room temperature, and thus thermal comfort was achieved.

4. CONCLUSIONS AND FUTURE WORKS

In this paper, mashrabiya performance was evaluated in detail by using the CFD ANSYS FLUENT 18.1. The simulation started by creating a benchmark model that was validated based on wind tunnel experiment data of the PIV and CFD reference. After that, two main stages of simulations were conducted to achieve the aim of this work: 1) the base case, which included the mashrabiya, 2) heat transfer devices combined with mashrabiya.

The results of the base case of mashrabiya generally contributed to increasing the proportion of airflow into the room, while the slats' angle played an efficient role in the direction of the airflow into the room. Also, the results indicated the efficiency of adopted heat transfer devices where the thermal comfort was enhanced significantly with applying double pipes. Overall, the applied technique decreased the temperature by one degree (2.5%) with single row pipes compared to 7.5°C (18.8%) with double rows pipes where the thermal comfort was achieved.

This study was limited to investigating the air velocity and temperature without including other prime functional values as daylight. Therefore, daylight should be investigated to provide a comprehensive optimal design of the mashrabiya. In addition, the investigation

of the effect of mashrabiya was limited to one type and design while study more different designs and sizes will be useful. Finally, future works are needed to create an actual model and conducting fieldwork will be advantageous to confirm the reliability of the proposed design in the simulation.

ACKNOWLEDGEMENT

The first author gratefully acknowledges the Saudi Arabian Cultural Bureau (SACB) in the United Kingdom and the scholarship sponsored by Umm Al-Qura University for financially supporting this research.

REFERENCES

[1] A. A. Bagasi and J. K. Calautit, "Experimental field study of the integration of passive and evaporative cooling techniques with Mashrabiya in hot climates," *Energy and Buildings,* vol. 225, p. 110325, 2020/10/15/ 2020, doi: https://doi.org/10.1016/j.enbuild.2020.110325.

[2] A. A. Maghrabi, "Airflow characteristics of modulated louvered windows with reference to the Rowshan of Jeddah, Saudi Arabia," Doctor of Philosophy, School of Architecture, University of Sheffield, Sheffield, UK, 2000. [Online]. Available: http://etheses.whiterose.ac.uk/id/eprint/14623

[3] T. Nakanishi, T. Nakamura, Y. Watanabe, K. Handou, and T. Kiwata, "Investigation of Air Flow passing through Louvers," *Komatsu Technical Report 2,* vol. 53, no. 160, 2007. [Online]. Available: https://www.semanticscholar.org/paper/Investigation-of-Air-Flow-passing-through-Louvers-Nakanishi-Nakamura/38a0b46f7271f182fa45e8084e1a8586772986b6.

[4] K. Kosutova, T. van Hooff, C. Vanderwel, B. Blocken, and J. Hensen, "Cross-ventilation in a generic isolated building equipped with louvers: Wind-tunnel experiments and CFD simulations," *Building and Environment,* vol. 154, pp. 263-280, 2019/05/01/ 2019, doi: https://doi.org/10.1016/j.buildenv.2019.03.019.

[5] C.-M. Chiang, N. Chen, P. Chou, Y. Li, and I. Lien, "A study on the influence of horizontal louvers on natural ventilation in a dwelling unit," in *The 10th International Conference on Indoor Air Quality and Climate*, 2005. [Online]. Available: https://www.pws.stu.edu.tw/paul/B_Conference/B100.pdf. [Online]. Available: https://www.pws.stu.edu.tw/paul/B_Conference/B100.pdf

[6] S. Di Turi and F. Ruggiero, "Re-interpretation of an ancient passive cooling strategy: a new system of wooden lattice openings," *Energy Procedia,* vol. 126, no. 201709, pp. 289-296, 2017/09/01 2017, doi: https://doi.org/10.1016/j.egypro.2017.08.159.

[7] M. M. Elwan, "The role of traditional Lattice window" Mashrabiya" in delivering single-sided ventilation-A CFD Study," *International Journal of Engineering Trends and Technology (IJETT),* vol. 68, no. 9, 2020, doi: 10.14445/22315381/IJETT-V68I9P221.

[8] R. Ramponi and B. Blocken, "CFD simulation of cross-ventilation for a generic isolated building: Impact of computational parameters," *Building and Environment,* vol. 53, pp. 34-48, 2012/07/01/ 2012, doi: https://doi.org/10.1016/j.buildenv.2012.01.004.

[9] J. K. Calautit, D. Connor, P. Sofotasiou, and B. R. Hughes, "CFD Simulation and Optimisation of a Low Energy Ventilation and Cooling System," *Computation,* vol. 3, no. 2, pp. 128-149, 2015, doi: https://doi.org/10.3390/computation3020128.

[10] C. Shen and X. Li, "Solar heat gain reduction of double glazing window with cooling pipes embedded in venetian blinds by utilizing natural cooling," *Energy and Buildings,* vol. 112, pp. 173-183, 2016, doi: https://doi.org/10.1016/j.enbuild.2015.11.073.

[11] J. Franke, A. Hellsten, H. Schlünzen, and B. Carissimo, "Best Practice Guideline for the CFD Simulation of Flows in the Urban Environment," *COST Office Brussels,* vol. 732, p. 51, 2007.

[12] Y. Tominaga *et al.*, "AIJ guidelines for practical applications of CFD to pedestrian wind environment around buildings," *Journal of Wind Engineering and Industrial Aerodynamics,* vol. 96, no. 10, pp. 1749-1761, 2008/10/01/ 2008, doi: https://doi.org/10.1016/j.jweia.2008.02.058.

[13] ASHRAE, "ANSI/ASHRAE Standard 55," in *Thermal Environmental Conditions for Human Occupancy*, 2010.

[14] J. K. Calautit, H. N. Chaudhry, B. R. Hughes, and S. A. Ghani, "Comparison between evaporative cooling and a heat pipe assisted thermal loop for a commercial wind tower in hot and dry climatic conditions," *Applied Energy,* vol. 101, pp. 740-755, 2013/01/01/ 2013, doi: https://doi.org/10.1016/j.apenergy.2012.07.034.

[15] R. J. de Dear and G. S. Brager, "Thermal comfort in naturally ventilated buildings: revisions to ASHRAE Standard 55," *Energy and Buildings,* vol. 34, no. 6, pp. 549-561, 2002/07/01/ 2002, doi: https://doi.org/10.1016/S0378-7788(02)00005-1.

[16] J. F. Nicol and M. A. Humphreys, "Adaptive thermal comfort and sustainable thermal standards for buildings," *Energy and Buildings,* vol. 34, no. 6, pp. 563-572, 2002/07/01/ 2002, doi: https://doi.org/10.1016/S0378-7788(02)00006-3.